

Multi-Agent Collaboration for Automated Design Exploration on High Performance Computing

Harshitha Menon¹, Charles F. Jekel¹, Kevin Korner¹, Brian Gunnarson¹, Nathan K. Brown², Michael Stees¹, M. Giselle Fernandez-Godino¹, Walter Nissen¹, Meir H. Shachar¹, Dane M. Sterbentz¹, William J. Schill¹, Yue Hao¹, Robert Rieben¹, William Quadros², Steve Owen², Scott Mitchell², Ismael D. Boureima³, Jonathan L. Belof¹

¹*Lawrence Livermore National Laboratory*

Emails: {harshitha, jekel1, korner1, gunnarson1, stees1, fernandez48, nissen5, shachar1, sterbentz2, schill1, hao1, rieben1, belof1}@llnl.gov

²*Sandia National Laboratories*

Emails: {nkbrown, wrquadr, sjowen, samitch}@sandia.gov

³*Los Alamos National Laboratory Los Alamo*

Emails: iboureima@lanl.gov

Abstract—Today’s scientific challenges, from climate modeling to Inertial Confinement Fusion design to novel material design, require exploring huge design spaces. In order to enable high-impact scientific discovery, we need to scale up our ability to test hypotheses, generate results, and learn from them rapidly. We present MADA (Multi-Agent Design Assistant), a Large Language Model (LLM) powered multi-agent framework that coordinates specialized agents for complex design workflows. A Job Management Agent (JMA) launches and manages ensemble simulations on HPC systems, a Geometry Agent (GA) generates meshes, and an Inverse Design Agent (IDA) proposes new designs informed by simulation outcomes. While general purpose, we focus development and validation on Richtmyer–Meshkov Instability (RMI) suppression, a critical challenge in Inertial Confinement Fusion. We evaluate on two complementary settings: running a hydrodynamics simulations on HPC systems, and using a pre-trained machine learning surrogate for rapid design exploration. Our results demonstrate that the MADA system successfully executes iterative design refinement, automatically improving designs toward optimal RMI suppression with minimal manual intervention. Our framework reduces cumbersome manual workflow setup, and enables automated design exploration at scale. More broadly, it demonstrates a reusable pattern for coupling reasoning, simulation, specialized tools, and coordinated workflows to accelerate scientific discovery.

Index Terms—multi-agent systems, large language models, high performance computing, scientific workflows, design optimization

I. INTRODUCTION

Scientific discovery increasingly depends on exploring vast design spaces that are too large and complex for manual exploration. From fusion energy research to novel materials discovery, progress requires rapidly testing hypotheses, generating results, and learning from them at scale. Although high-performance computing (HPC) has made it possible to simulate physics with high fidelity, but simply running larger simulations is not sufficient. What is needed are closed-

loop workflows that tightly integrate simulation, analysis, and design exploration.

Today, however, most design workflows are cumbersome and heavily manual. Exploring large parameter spaces under strict physical and engineering constraints requires moving through an expensive cycle of design, simulation, validation, and analysis. Although workflow management systems [1]–[3] automate job execution and data movement, they still place a significant manual burden on scientists. In particular, they must explicitly construct workflow graphs, define how simulations are executed, and specify exploration strategies. As a result, researchers spend much of their effort managing orchestration logic rather than advancing the underlying scientific objectives. Moreover, as scientific problems continue to grow in scale and complexity, such approaches become increasingly difficult to sustain. Consequently, we need automated and efficient design workflows to advance frontier science and accelerate the pace of discovery.

Large Language Models (LLMs) have shown impressive capability in several domains, from natural language understanding and code generation to planning and problem solving [4]–[6]. Their ability to reason over complex information makes them attractive to scientific applications [7]–[9]. However, the best way to leverage LLMs for complex scientific and engineering tasks remains an open question.

We propose MADA (Multi-Agent Design Assistant), a multi-agent framework powered by LLMs and integrated with domain-specific tools. The framework modularizes the scientific design workflow into specialized agents, each responsible for different stages of the scientific workflow. Within this framework, LLMs act as reasoning engines that guide collaboration by analyzing results, extracting insights, and adapting workflows as the context evolves. As opposed to requiring scientists to manually configure simulations, manage job submissions, and interpret results, MADA shifts these

responsibilities to agents. Importantly, agents not only execute the workflow, but also use the insights to drive the next round of design iterations. The framework consists of several specialized agents orchestrated by a planning component that coordinates cycles of design, simulation, and analysis. Specifically, the Job Management Agent (JMA) handles large ensembles of jobs on HPC systems, the Geometry Agent (GA) automates mesh generation and validation, and the Inverse Design Agent (IDA) explores the design space, guided by simulation results. Together, these agents transform what has traditionally been a cumbersome, manual workflow into an automated, modular, and scalable approach to scientific design exploration.

While the framework is general purpose, we demonstrate its capabilities on Richtmyer–Meshkov Instability (RMI) suppression problem [10], a critical challenge in Inertial Confinement Fusion (ICF) research. RMI occurs when shock waves amplify perturbations at material interfaces, causing jet-like growths that can degrade the capsule and prevent successful fusion ignition. We evaluate our system in two complementary settings. In the first, MADA drives the full design loop, generating meshes, launching and managing simulation runs on HPC systems, and analyzing outputs to discover interface geometries that suppress RMI. In the second, agents use a pre-trained machine learning surrogate model for rapid design exploration. Together, these evaluations demonstrate the framework’s flexibility to support diverse computational backends.

The primary contributions of this paper are as follows:

- MADA, a multi-agent framework that coordinates end-to-end scientific design exploration on HPC systems. The framework decomposes the design loop into specialized agents that handle mesh generation, job orchestration, and inverse design, thereby supporting automated workflows.
- Three specialized agents for scientific computing: a Job Management Agent for submitting and monitoring simulation ensembles via Flux [11], a Geometry Agent for automated mesh generation through Cubit [12], and an Inverse Design Agent for design space exploration guided by simulation results.
- Integration with existing HPC tools and infrastructure via the Model Context Protocol [13], which allows agents to directly call domain-specific tools.
- An evaluation of RMI suppression demonstrating iterative design refinement using Laghos [14] hydrodynamics simulations on HPC, and surrogate-based optimization [15] where the agent found good designs quickly while providing interpretable reasoning.

Our work demonstrates how multi-agent workflows that combine LLM reasoning with direct tool integration can accelerate scientific discovery by reducing orchestration overhead and supporting efficient exploration of complex design spaces.

II. BACKGROUND

Large Language Models (LLMs) have demonstrated remarkable capabilities in understanding and generating human

language, code, and structured reasoning [4], [5], [16]. As a result, recent advances have shown that LLMs can serve as powerful reasoning engines for complex tasks that require planning, tool use, and multi-step problem-solving [6], [17], [18]. In scientific computing contexts, LLMs provide a natural interface between human intent and computational workflows, translating high-level objectives into executable actions [7]. Moreover, their ability to understand context, maintain state across interactions, and adapt to feedback makes them well-suited for orchestrating scientific workflows that traditionally required extensive manual oversight [9], [19].

A. Agents and Tool Use

An LLM-based agent is an autonomous entity that perceives its environment, makes decisions, and takes actions to achieve specific goals [20]. In the context of LLMs, agents extend the base model’s capabilities by integrating external tools, accessing real-time information, and executing actions in computational environments [21]–[23]. As a result, the agent paradigm transforms LLMs from passive question-answering systems into active problem solvers that can interact with simulations, manage computational resources, and iterate on solutions [24], [25]. A key characteristic of LLM-based agents is tool integration, which allows agents to call specialized tools for tasks beyond the LLM’s native capabilities, including running simulations, generating meshes, or analyzing data [26], [27]. In addition, agents maintain memory and state across interactions, allowing them to track progress, learn from previous results, and adapt strategies [18], [28]. Furthermore, agents exhibit goal-directed behavior by decomposing high-level objectives into actionable subtasks and executing them systematically [29], [30].

B. Multi-Agent Systems

While single agents can be effective for narrowly scoped tasks, complex scientific workflows often require diverse expertise and parallel execution capabilities that exceed what a single agent can efficiently manage [31], [32]. Multi-agent systems address this by orchestrating multiple specialized agents that collaborate to solve larger problems [33]–[35]. Each agent focuses on its area of expertise while contributing to the collective goal [36], [37]. Multi-agent architectures offer several advantages. First, specialization allows each agent to be optimized for specific tasks, improving overall system performance and reliability [31]. Second, modularity makes it possible to add new agents or modify existing ones without disrupting the whole system [33]. Third, distributing responsibilities across multiple agents helps manage the limited context windows of LLMs. By assigning distinct subtasks to specialized agents, each agent can operate within a focused and relevant context, reducing information overload. Finally, this division of labor improves robustness, as failures in one agent do not necessarily compromise the entire workflow. Instead, other agents can adapt or compensate as needed [38].

C. Model Context Protocol (MCP)

The Model Context Protocol (MCP) is an open standard that enables seamless integration between LLMs and external tools [13]. MCP follows a client-server architecture with three roles: the *host* is the AI application that coordinates connections, the *client* maintains a stateful session with a single server, and the *server* exposes capabilities to clients. Communication uses JSON-RPC 2.0 over standard input/output for local servers or Streamable HTTP for remote servers.

Servers expose three types of primitives. First, *Tools* correspond to executable functions that the LLM can invoke, such as submitting a job or generating a mesh. Second, *Resources* provide contextual data like file contents or database records. Third, *Prompts* offer reusable templates for LLM interactions. During initialization, clients and servers exchange capability negotiation through a handshake, allowing clients to discover available tools and servers to advertise their features.

Within our framework, MCP therefore serves as the communication backbone between agents and our tools. Rather than modifying these tools, we expose their functionality through lightweight MCP servers. In particular, each MCP server wraps a specific tool, such as Flux, simulation code, Cubit, surrogate models, and provides a standardized interface that agents can query. This separation means agents written for one MCP-compliant tool work with any other compliant tool without any modification.

III. MADA SYSTEM OVERVIEW

Modern scientific discovery requires solving problems that a single tool or agent cannot address alone. While a single agent can effectively handle narrow, well-bounded tasks such as answering queries, retrieving data, or performing basic calculations, it quickly becomes overloaded when faced with complex, multi-step workflows. Scientific workflows is one such scenario, demanding diverse skill sets, long-horizon reasoning, and coordination across various environments such as simulation code, domain-specific tools, and HPC systems.

The main goal of MADA is to automate iterative scientific design loop, which includes proposing candidate designs, generating meshes, running simulations, analyzing results, and refining. To support this process, MADA uses a set of specialized agents, each responsible for a distinct role in the workflow (Figure 1). The Job Management Agent (JMA) handles simulation execution on HPC systems, the Geometry Agent (GA) produces meshes, and the Inverse Design Agent (IDA) analyzes results and proposes new candidates. These agents access external tools through the Model Context Protocol (MCP) (Section II), which provides a uniform interface for tool discovery and invocation.

A typical design exploration proceeds as follows. The user specifies the objective (e.g., suppress RMI), design variables (e.g., interface geometry parameters), and constraints (e.g., parameter bounds). Next, the GA generates the corresponding problem mesh. The IDA then produces an initial batch of candidate designs, either through broad exploration or targeted sampling near promising regions. For each candidate, the JMA

submits the simulation. Once the results return, IDA extracts quantities of interest, ranks configurations, and proposes the next batch. This cycle repeats until the user terminates or a convergence criterion is met.

More broadly, we build our framework around five core components:

- **Specialized Agents:** Agents responsible for different stages of the scientific workflow.
- **Planning:** A planning component decomposes high-level scientific goals into subtasks.
- **Coordination:** Agents communicate through well-defined interfaces to schedule work and share results.
- **Tool Integration:** MCP expose specialized scientific tools (mesh generators, simulation codes, HPC schedulers) through a standardized interface for agent interaction.
- **Memory:** Results and context persist to make possible continuous improvement over iterative design cycles.

1) *Specialized Agents:* The JMA interfaces with simulation codes and schedules job ensembles on HPC systems. It communicates with Flux [11] through an MCP server, submitting jobs, monitoring execution, and reporting outcomes. The Inverse IDA drives optimization and design-space exploration. It interfaces with surrogate models for rapid evaluation, computes quantities of interest, and proposes new candidate designs based on simulation results. The GA automates mesh generation from user specifications. It interfaces with Cubit [12] or PMesh [39] to produce simulation-ready meshes.

2) *MADA Orchestration and Agent Coordination:* MADA orchestrates complex scientific workflows by converting high-level user objectives into executable plans and coordinating them across various agents. Unlike traditional workflow management systems that require explicit specification of every step, MADA uses LLM-based reasoning to dynamically decompose tasks, allocate work to appropriate agents, and adapt the execution strategy based on intermediate results.

We implement MADA on top of the AutoGen framework [33], which is platform for building multi-agent applications. Figure 2 illustrates the multi-agent coordination process. The coordination happens in three stages. First, a context analyzer consolidates the conversation history and agent capabilities. Next, a selector uses this context to determine which agent should act next—this decision adapts to the current workflow state rather than following a fixed sequence. Finally, the selected agent produces a response, often invoking one or more tools, and shares a summarized result with all agents. As a result, the entire system maintains a consistent view of the workflow state. When an agent fails or encounters unexpected behavior, the system adapts by adjusting the subsequent actions.

3) *Tool Integration via MCP:* We wrap each tool (Flux, Cubit, simulation code, surrogate models) in an MCP server that exposes its functionality through a standardized interface. We configure agents to connect to specific servers, discover available capabilities, and invoke tools by sending structured requests. MCP handles parameter validation, error reporting, and result formatting. This separation between agent logic and

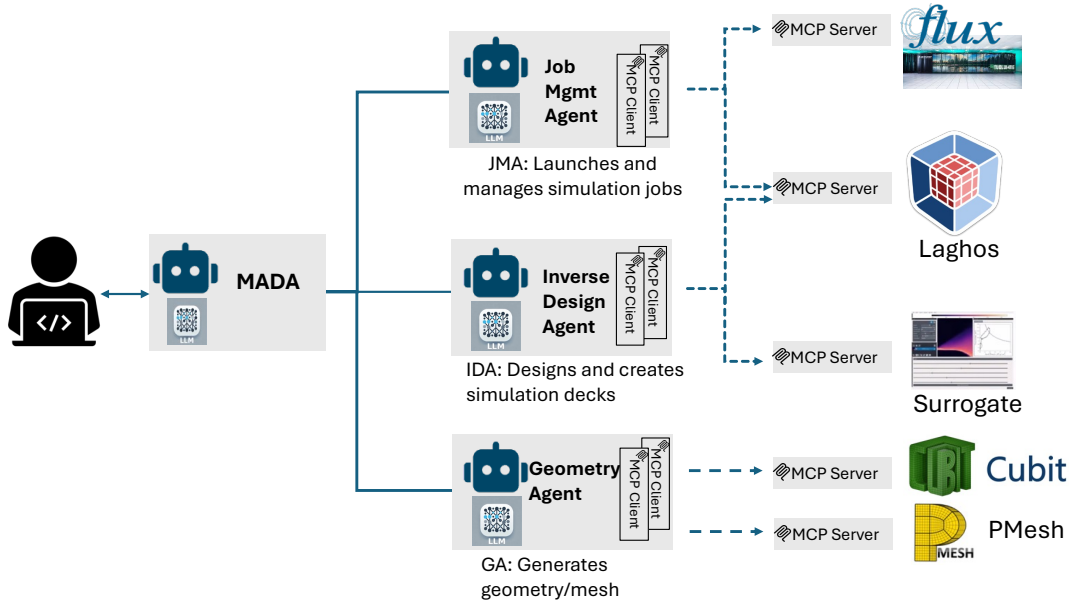


Fig. 1. MADA system architecture. The framework orchestrates three specialized agents: the Job Management Agent (JMA) manages simulations on HPC via Flux, the Geometry Agent (GA) generates meshes through Cubit, and the Inverse Design Agent (IDA) explores the design space. Agents communicate with tools via the Model Context Protocol (MCP).

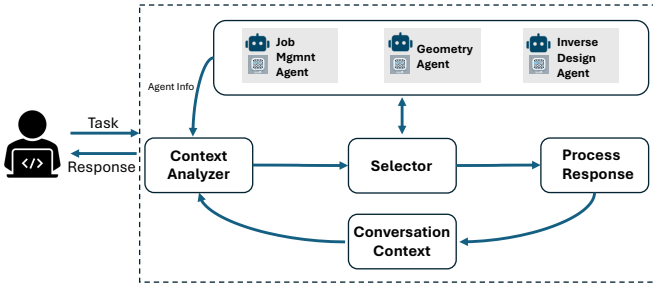


Fig. 2. Coordination process. The context analyzer processes conversation history and agent roles. The selector chooses the next speaker. The selected agent responds, and the system broadcasts the message to maintain shared state. This cycle repeats until the system reaches termination.

tool implementation means that an MCP-compliant tools can interoperate with any other MCP-compliant agentic framework.

A. Job Management Agent (JMA)

The JMA interfaces with simulation codes and ensures reliable execution of large simulation ensembles on HPC systems. It abstracts the complexity of interacting with schedulers like Flux and provides a robust interface to launch, monitor, and collect simulation results.

The JMA utilizes two key types of MCP servers: simulation codes and schedulers. The simulation code MCP servers define what to run, while the scheduler MCP servers define how to execute the jobs that simulation codes specify.

We designed the JMA so that users can easily integrate additional job scheduler MCP servers (for example, Slurm, Merlin, or Parsl) and other simulation codes. A JSON config-

uration file configures the JMA, GA, and IDA by pointing each agent to the appropriate MCP servers. For the JMA, this currently means Laghos for simulation and Flux for job scheduling. To support a new scheduler or code, users add a corresponding MCP server entry to this configuration file if one already exists, or wrap the tool in a new MCP server.

1) Simulation Code Interface:

a) *Laghos*: Laghos (LAGrangian High-Order Solver) [40] is an open-source miniapp code derived from MARBL [41] that solves the time-dependent Euler equations of compressible gas dynamics in a moving Lagrangian frame using unstructured high-order finite-element spatial discretization and explicit high-order time stepping.

In this work, we employ Laghos3 [42], the differentiable extension of Laghos with the following extensions:

- Support for complex material models, such as Mie-Grüneisen equations of state
- A unified interface for specifying initial conditions, boundary conditions, and geometries
- Configuration of problem setups through Lua-based input decks

These enhancements enable fine-grained, programmatic control of problem configuration and parameters via the JMA. The Lua-based configuration is particularly useful for agentic workflows: the JMA can pass new parameters at runtime without needing to recompile the application for each exploration.

We expose Laghos functionality through an MCP server that provides tools for staging and configuring simulations. The primary tool, `generate_runs()`, takes a set of design parameters and generates the corresponding simulation input files, including Lua configuration decks and stages them for

execution. This tool returns a list of run descriptions that the JMA can pass to the Flux scheduler for execution. In this design, the JMA delegates application configuration and staging to application-specific MCP server and then forwards the resulting run descriptions to a scheduler-specific MCP server, thereby maintaining a clear separation of concerns.

2) *Scheduler Integration*: We architected the JMA for modular scheduler integration. The JMA abstracts scheduler-specific logic behind a unified interface, allowing users to switch between job schedulers and extend to new ones without disrupting existing workflows. This modular design supports scalable simulation workflows across diverse HPC environments.

Currently, the JMA supports the Flux job scheduler for managing jobs. Flux is a next-generation, hierarchical resource management and job scheduling framework developed for HPC systems [11]. It provides a flexible and composable scheduling architecture that supports dynamic partitioning and allocation of resources across multiple nested scheduling domains. By treating scheduling as a distributed service, Flux enables fine-grained control, rapid job dispatch, and efficient resource utilization on systems ranging from clusters to exascale supercomputers. Its modular design, rich APIs, and integration with modern computing environments make it a robust foundation for advanced workload management and experimentation.

Flux integration is implemented as an MCP server that exposes a set of MCP tools built using the Python bindings of Flux. The server provides four key MCP tools: `submit_job()`, `submit_jobs_async()`, `check_job_status()`, and `execute_generated_runs()`. The `submit_job()` tool submits a single command to the Flux scheduler, allowing users to specify basic resource requirements such as the number of nodes, tasks per node, time limit, job name, and working directory, and returns the corresponding Flux job ID. The `submit_jobs_async()` tool accepts a JSON description of multiple runs and submits them asynchronously, immediately returning job identifiers so that large ensembles or parameter sweeps can be launched without blocking. The `check_job_status()` tool queries the scheduler for the state of a given job, or all managed jobs if the user provides no ID, and returns a JSON summary of their current status. Finally, `execute_generated_runs()` takes generated run descriptions (for example, from the Laghos MCP server) and executes them synchronously, submitting and monitoring each run until completion and returning a textual summary of their outcomes.

B. Geometry Agent (GA)

The GA automates geometry generation and mesh preparation for candidate designs by translating plain-text CAD descriptions into the corresponding of the user’s choice of two modeling and mesh generation packages: Sandia National Laboratories’ Cubit, and Lawrence Livermore Laboratories’ PMesh.

1) *Interacting with Cubit*: Cubit is Sandia National Laboratories’ flagship geometry-creation and mesh-generation tool. It is used to build solid models (points, lines, surfaces, volumes) and to produce high-quality finite-element meshes. Cubit is typically used early in the analysis pipeline: engineers create the physical model, generate a mesh that satisfies the physics-specific resolution criteria, and then export the mesh to the downstream solver.

Users traditionally interact with Cubit in one of three ways: 1. Graphical user interface for interactive CAD modeling and mesh generation, 2. Native command-line scripting with Cubit’s domain-specific language (DSL), 3. Programmatically using the Python API that wraps those commands for automated workflows. We will primarily focus on the Python API here.

The Cubit Python API exposes a thin wrapper around Cubit’s native command language, allowing Python scripts to issue the same geometry-creation and mesh-generation commands that are normally achieved interactively in the Cubit interface. Internally, the API parses the DSL, consisting of high-level commands (e.g. “create vertex”, “block x_dim y_dim z_dim”, “mesh volume X”) translating them into Cubit’s tool command language-based instruction set. Because the DSL is interpreted by the Python layer, users can embed conditional logic, loops, and external data sources directly in their scripts, enabling fully automated, reproducible design and mesh pipelines that integrate seamlessly with other Python-based analysis tools. Because the DSL is accessible through a standard Python interface, the GA is strategically situated to generate or execute Python code that can drive Cubit in real time. By formulating appropriate DSL statements and issuing them via the API, the GA can create geometry, apply mesh controls, and retrieve mesh quality metrics while only requiring human interaction through natural language prompting.

2) *Interacting with PMesh*: PMesh is Lawrence Livermore’s massively parallel CAD-based mesher for multi-physics HPC simulation. While CUBIT has extensive CAD creation and unstructured mesh generation, PMesh focuses on precise control over mesh structure and resolution while generating meshes of billions of elements. All scripting is done through its Python API, which is similar to Cubit’s. The output is an MFEM-formatted [43] cubic NURBS mesh, suitable for simulation as-is, or able to be refined in parallel with no loss of accuracy.

3) *Leveraging Cubit Documentation via RAG*: The GA relies on a Retrieval-Augmented Generation (RAG) pipeline that draws from a curated knowledge base containing the Cubit user-documentation and a collection of vetted example scripts. Each user-manual section was pre-processed into discrete text chunks, each encapsulating a one–three DSL function names, concise descriptions of purpose and parameters, and representative usage examples. This granularity limits context overload and ensures that every retrieved fragment supplies the essential “ground-truth” syntax and semantics needed to translate a natural-language CAD request into the correct Cubit

DSL commands.

When a user submits a task, the GA first embeds the request using a vector-encoding model and then computes cosine similarity between this query vector and the vectors of all documentation chunks. The top N most similar fragments, typically those with similarity scores above a calibrated threshold, are selected and concatenated into the prompt supplied to the language model. By presenting the model with the most relevant function definitions and examples, the RAG step guides generation toward syntactically correct and semantically appropriate DSL, while still allowing the model to reason about higher-level iterative logic.

4) *Leveraging PMesh Documentation via RAG:* When using the PMesh option, the GA draws from a similar corpus of documentation. PMesh’s documentation is entirely programmatically generated via introspection, allowing trivial chunking of each semantic function. In addition to a ChromaDB [44] vector database search using cosine similarity as described in the previous section, we introduce hybrid search by including keyword matches based on textual similarity using Bm25 [45]. Each of the over 1500 documented function points follows a consistent structure: Python syntax declaration, a “one-liner” high-level description, names and types of positional and keyword arguments, extended prose description, and one or more examples (tested nightly as part of a continuous integration (CI) pipeline). This aids the LLM in selecting an appropriate API based on the purpose of the query, as well as providing executable code snippets to use and modify.

5) *Capturing Spatial and Geometric Information:* A critical aspect of any CAD modeling task is the ability to understand the geometric and spatial attributes of the present model. Achieving such an understanding with an LLM is a non-trivial task. Previous works have shown vision language models are able to provide limited understanding of a CAD model, but commonly suffer from significant information loss when the CAD views are not sufficiently detailed [46], [47]. Therefore, we leverage a topological approach to feed general geometric and spatial information into the GA. We construct a geometric graph that encodes the complete topology of the active Cubit model. Each node in the graph corresponds to a fundamental entity (i.e. vertex, edge, surface) and is enriched with attribute fields that capture its quantitative description. For a vertex node we store its Cartesian coordinates, for an edge node we record its length, centroid coordinates, and mesh size/intervals, and finally surface nodes define centroid coordinates, area, outward normal vector and mesh size/intervals. The graph edges represent the incidence relationships: a vertex node is linked to every edge node that uses it, an edge node connects to the surface nodes that contain it. This explicit connectivity preserves the full topological hierarchy without requiring additional inference.

After the graph is assembled, we serialize it into a structured textual representation that lists each entity together with its attributes and adjacency lists. The format follows a consistent schema, ensuring that the language model can parse the data deterministically. This structured block is then inserted into

the system prompt of the GA, providing the LLM with an up-to-date snapshot of the model’s geometry and topology. With this information readily available, the GA can generate precise Cubit DSL commands, resolve spatial queries (such as “find the nearest surface to vertex 5”), and make informed decisions about geometry modifications or mesh refinements.

6) *Tackling Specialized Design Tasks via Tool Calling:* The GA is equipped with an agentic tool-calling capability that lets it invoke specialized functions and external utilities on demand to tackle complex or specialized design, model preparation, or mesh tasks. Such tools include invoking external knowledge sources to parametrically define, design, mesh, and export 2D shaped charges, drastically accelerating the model generation of a traditionally time consuming component. Additionally, for defeaturing operations, the GA can invoke Cubit’s built-in “power tools”, which are accessed directly through the Python API. When the user requests model preparation tasks, such as removing small cavities or fillets, the agent calls the appropriate power-tool functions while modifying parameters according to the user prompt. The tool-calling framework is extensible: new capabilities can be registered whenever a user supplies additional resources, such as custom Python modules or domain-specific instruction sets. The GA queries the availability of each tool at runtime, falls back to alternative methods if a required utility is absent, and updates its output based on tooling outcomes. This dynamic integration ensures that the GA can adapt to evolving workflow requirements while maintaining a consistent, reproducible pipeline for complex CAD tasks.

7) *Verification and Iteration:* In the system prompt, we explicitly instruct the GA “do not suggest incomplete code which requires others to modify”. This is more likely to produce a correct executable result, rather than a chatbot-style conversational response that assumes the user will be copy-pasting into another context. To test the quality of this response, we execute it within Cubit or PMesh and verify the result. In Cubit we use a simple axis-aligned bounding box to assess approximate geometric congruence with a human-generated reference result. We also compare the textual similarity of the response to a human-generated reference command script. To test a PMesh result we generate a best-match bijection that uses topological correspondence (vertex count, connectivity) as well as approximate geometric congruence (maximum distance). In particular, we do not penalize the GA for producing additional geometry, or proceeding further than requested, such as mesh generation.

When tool calls or generated commands fail to produce the reference result, which is inevitable, clear and specific error messages are essential. In cases where the initially provided context was insufficient, reporting a simple syntax error can prompt the GA to retrieve new, hopefully more relevant context. Similarly, reporting that the geometry deviated from the desired result may allow the GA to go back and attempt to correct its error.

The GA is designed as a fast, reliable agent that can generate, mesh, and iteratively refine CAD models on demand,

providing a consistent source of high-quality geometry for downstream processes. Since it supports two different and complementary mesh generators, the user can pick the best one for the task, without changing their prompt. Integrated into the broader MADA workflow, the GA can be invoked directly by users or called by other agents, enabling seamless agent-to-agent collaboration that continuously checks and improves design and mesh quality to meet a wide array of digital design objectives.

C. Inverse Design Agent (IDA)

The primary job of IDA is optimization and design-space exploration. It analyzes simulation results and, when available, uses surrogate models to propose new candidate designs. The IDA calculates quantities of interest (QoI) from simulation outputs that is used to guide design decisions. For RMI suppression problems, the QoI is jet length, which measures the extent of material jetting at the perturbed interface. When working with full hydrodynamics simulations, the IDA extracts jet length from tracer diagnostics in the simulation output. When using surrogate models, it computes jet length from the predicted density fields. The IDA ranks candidate designs by their QoI values and identifies configurations that best meet the design objectives.

The IDA interfaces with machine learning surrogate models for rapid design exploration. These surrogate models approximate the simulation response at a fraction of the computational cost. The IDA queries the surrogate at random points of the parameter space, computes QoI from predicted fields, and analyzes results using LLM-based reasoning to propose promising new configurations.

The IDA connects to two types of MCP servers depending on the evaluation mode. For simulations, the IDA connects to an application-specific MCP server that exposes tools to calculate QoI from simulation outputs. For example, the Laghos MCP server provides `get_qoi()`, which extracts jet length from tracer diagnostics. For surrogate-based exploration, the IDA connects to a surrogate model [15] MCP server that exposes `get_objective()`, which runs inference and computes objective values for a given design input. This separation allows us to swap evaluation backends without modifying the IDA logic, and lets the IDA use HPC simulations when accuracy is critical or fast surrogate models to efficiently explore large design spaces.

D. Expert-in-the-Loop with MADA

Although MADA can operate autonomously, the domain experts can play a role in guiding the design exploration process. MADA supports expert-in-the-loop interaction via two interfaces. A command-line interface (CLI) lets experts interact with MADA directly from a terminal, suitable for HPC environments where graphical interfaces may not work. We also provide a graphical user interface (GUI) that displays simulation results, optimization progress, and agent reasoning. Through both the CLI and GUI, experts can interact at multiple stages of the workflow. At the start of the exploration, experts

specify design objectives, constraints, and variable ranges. During execution, they may review intermediate results, adjust search parameters, and redirect the exploration based on their domain knowledge. At the end of each iteration, experts can evaluate the designs that MADA proposes and decide whether to continue refining, explore other strategies, or terminate the study.

This interaction model combines the strengths of automated exploration with human expertise. On one hand, MADA agents handle the burden of mesh generation, job submission, and result analysis. On the other hand, the experts provide high-level guidance and interpret results in the context of broader scientific goals. Moreover, the natural language interface allows experts to communicate intent without writing code or configuring complex workflow scripts. As a result, this collaboration helps MADA to leverage expert intuition and domain knowledge while performing design exploration.

IV. EVALUATION AND CASE STUDIES

We evaluate MADA on the task of studying Richtmyer–Meshkov Instability (RMI) [10], a critical problem in Inertial Confinement Fusion (ICF) research. RMI occurs when a shock wave amplifies perturbations at a material interface, causing large jet-like growths [48]–[51]. When a shock wave reaches interface perturbations, vorticity deposition occurs along the interface due to misalignments between pressure and density gradients. This generally results in jetting of the target material. Understanding and controlling RMI is critical in many applications. For instance, experimental measurements of RMI formations are used to calibrate high strain rate material models, and in ICF experiments, RMI can form within fuel capsules and degrade their integrity and the fuel purity sufficiently to prevent ignition [52].

To study this problem under realistic conditions, we use two complementary settings. First, MADA drives the full design loop by generating meshes, launching and managing Laghos hydrodynamics simulations [14] on HPC systems, and analyzing simulation outputs. This setting captures the complexity and constraints of production scientific workflows. However, large-scale simulations are computationally expensive, which limits the number of designs that can be explored. Therefore, in the second setting, agents use a pre-trained machine learning surrogate model [15] that approximates the simulation response. For instance, each Laghos run takes approximately 20 minutes to complete, whereas the surrogate model evaluates a design in a fraction of a second. Together, these two settings provide a comprehensive evaluation of the framework’s ability to support both high-fidelity simulation-driven discovery and fast, surrogate-based design exploration for RMI suppression.

We ran all our evaluation on Tuolumne, a system at Lawrence Livermore National Laboratory containing 1,152 nodes, each with 4th Generation AMD EPYC processors (96 cores), four AMD MI300A accelerators, and 512 GB of memory. The system delivers a peak performance of 294 petaflops and debuted at #10 on the November 2024 Top500

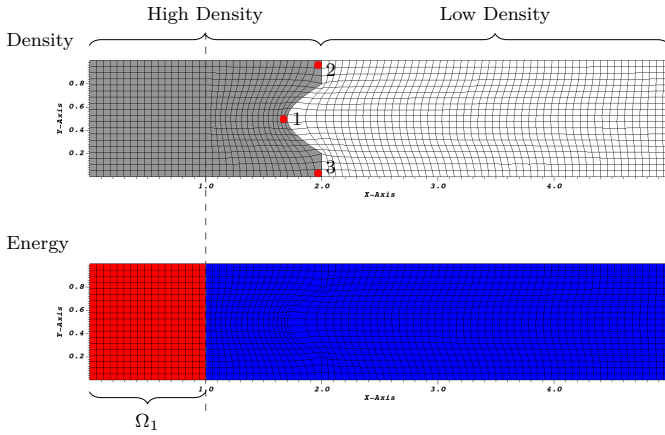


Fig. 3. Simulation setup of inertial confinement fusion in 2D with sinusoidal energy initialization in the x-axis and a perturbed interface to trigger RMI [42].

list. Tuolumne uses Flux [11] as its workload manager, a hierarchical resource manager designed for exascale workflows. All agents in MADA use OpenAI’s o3 reasoning model.

A. Design Exploration with Simulation

In this evaluation, we exercise the full design loop: specify design variables, generate meshes, run simulations, analyze results, and propose refinements.

For the problem of interest, we configure Laghos to simulate a Richtmyer–Meshkov instability (RMI) [10] using Mie-Grüneisen material models. In our setup, the computational domain consists of two materials, steel on the left and plastic on the right, separated by a sinusoidally perturbed interface. Within the steel, we designate a subregion as the design domain, where we control the initial energy distribution at runtime via parameters passed through the JMA. The prescribed energy profile in this design domain generates shocks that interact with the material interface and drive the development of the RMI. We treat all boundaries as sliding boundaries, which permit tangential motion along the boundary while preventing normal flow across it. We chose the setup shown in Figure 4 to study controllability of the interface evolution and, in particular, to investigate strategies for suppressing the growth of the RMI. Periodic diagnostic outputs from Laghos provide MADA with measurements of the instability length, enabling analysis of its dependence on the control parameters supplied by the JMA. We use the Laghos3 simulation code (Section III-A1a) to model shock propagation and RMI growth at the perturbed copper-plastic interface. The first region is initialized with a temperature profile characterized by a base internal energy of 0.1, to which sinusoidal perturbations along the x-axis are applied, subject to the constraint that local internal energy remains non-negative. The remaining domains are initialized with zero energy and velocity.

1) *Design Parameters and Objectives:* The goal of the optimization is to identify initial energy field configurations that minimize RMI growth while maximizing interface acceleration. Each design is parameterized by four values that

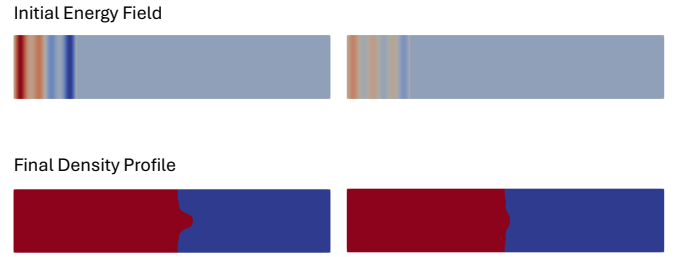


Fig. 4. Design exploration results for RMI suppression. Top row: initial energy field. Bottom row: final density profile. Left: configuration at the start of exploration (QoI = 4.1). Right: best design found by MADA (QoI = 3.7), showing significantly reduced jetting at the interface.

define the sinusoidal energy initialization along the x-axis, characterizing the perturbation applied to the density interface. The quantity of interest guiding the optimization is formulated as $QoI = 0.5\lambda_1(x_2 - x_{outer})^2 + \lambda_2/(\delta + |v_{ave}|)$, where x_2 denotes the deformed x-coordinate at the interface mid-height, $x_{outer} = 0.5(x_1 + x_3)$ represents the average position of the top (x_1) and bottom (x_3) interface points (providing a symmetric reference), and $v_{ave} = (v_1 + v_2 + v_3)/3$ is the mean x-velocity across these three monitoring points. The first term ($\lambda_1 = 30.0$) penalizes lateral displacement of the interface midpoint from its symmetric reference position, thereby suppressing perturbation amplitude growth characteristic of RMI. The second term ($\lambda_2 = 4.0$) inversely rewards higher interface velocities with regularization parameter $\delta = 1.0$ preventing singularities, thereby promoting configurations that enhance shock-driven acceleration.

2) *Workflow:* The user provides to MADA the problem description, the design parameters and their ranges via natural language. MADA parses this input and orchestrates workflow between the various agents. The GA generates a parameterized mesh template through Cubit. The IDA then produces a Latin hypercube sampling plan for initial exploration (20 samples). The JMA submits the ensemble to Tuolumne system via Flux and monitors job completion. As results return, the IDA extracts jet length from each run, ranks configurations, and identifies the best-performing design.

For the second round, the IDA narrows the search to a neighborhood around the current best and proposes additional samples. The cycle repeats: sample generation, job submission, result collection, analysis. At the end of each round, MADA reports a ranked table of configurations along with visualizations of the top designs. The user can request further refinement or stop. Over two exploration rounds, we evaluate 40 configurations. The best design reduced jet significantly as shown in Figure 4.

3) *Results:* In Round 1, MADA evaluates 20 Latin hypercube samples spanning the design space. The IDA analyzes the results and identifies configurations with lower QoI values, revealing that certain combinations of sinusoidal parameters consistently produce lower RMI growth. In Round 2, the IDA focuses sampling around the promising region from Round 1, evaluating 20 additional configurations.

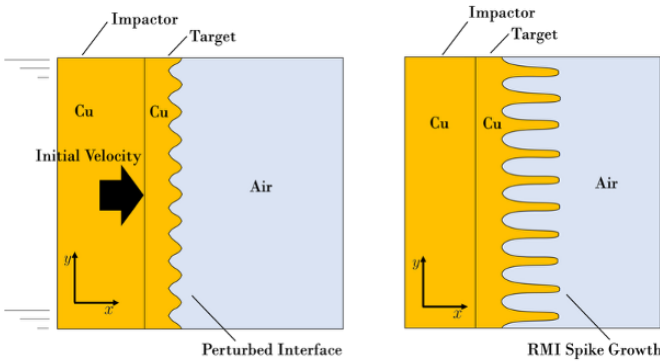


Fig. 5. Visualization of the high-velocity impact problem that results in the formation of RMI from [53].

Figure 4 shows the optimization results. The initial configuration yields a QoI of 4.1, while the best design MADA finds achieves a QoI of 3.7, representing a 10% improvement. The density field visualizations show reduced interface perturbation amplitude in the optimized configuration compared to the initial design.

The entire optimization completes in approximately 40 minutes, with simulations running in parallel. Without MADA, a domain expert would need to manually configure each simulation, monitor job completion, parse output files, and decide on the next sampling strategy, a process that typically takes days for comparable design studies. MADA reduces this burden on the expert by automating the scheduling and configuring part, thereby shifting expert effort toward scientific reasoning, interpretation, and discovery.

B. Design Exploration with Surrogate Model for High Velocity Impact

It is also possible to study RMI with the high velocity impact of two materials using a surrogate model from [15] in place of a high fidelity multi-physics simulation code [41], [54]. This approach enables rapid design exploration without the computational cost of running full hydrodynamics simulations, allowing MADA to evaluate hundreds of design configurations in seconds rather than hours. The underlying physics problem is a high velocity impact study that models a Cu flier plate moving at 2 km/s and impacting a Cu target with perturbations at the free surface of the target. As the shock wave reaches the interface perturbations, vorticity deposition occurs along the interface due to misalignments between pressure and density gradients. This creates a Richtmyer–Meshkov Instability (RMI) that results in jetting of the copper target material. The inputs to the surrogate model are four spline points that define the initial geometric perturbation on the free interface of the copper target. These spline points can be values in $[-0.25, 0.25]$ cm on the free interface of the copper target using piecewise cubic Hermite interpolating polynomial. Initial geometric perturbations, caused by the spline points having different values, result in RMI growth. In general, the larger the initial geometric perturbation, the larger

the resulting RMI. Likewise, when all four spline points are equivalent, there should be no initial geometric perturbation, resulting in little or no RMI growth. A depiction of this is shown in Figure 5.

It is possible to formulate an optimization problem on the surrogate to maximize RMI. Given this geometric setup, maximum RMI should occur when the spline points are at alternating extrema (e.g. $x = [-0.25, 0.25, -0.25, 0.25]$ or $x = [0.25, -0.25, 0.25, -0.25]$) as this creates the largest initial perturbation which seeds RMI growth. Likewise, the smallest RMI should occur when all of the spline points are set to the same value, which results in no initial perturbation. Typically this is done with numerical optimization techniques applied directly to the surrogate model. However, it is also possible to utilize an LLM agent to find what parameters minimize the RMI, which may offer several advantages. The agent provides interpretable reasoning about why certain configurations perform well, can transfer insights across similar problems, and interacts through natural language rather than requiring gradient information or custom code.

1) *Workflow*: The user provides MADA with a natural language description of the problem: the physical setup (high velocity impact of copper), the four spline parameters and their ranges ($P_i \in [-0.25, 0.25]$ cm), and the optimization objective (minimize or maximize RMI). Instead of submitting jobs to HPC, the IDA queries the surrogate model directly. The agent computes jet length from the predicted density field by identifying the minimum extent to which copper has penetrated into the air region.

2) *Results*: MADA performs three rounds of refinement: an initial sample of configurations, followed by two refinement rounds, for nearly 30 total evaluations with approximately 10 evaluations each round. Each round completes in a few seconds. The IDA analyzes results after each round, identifies promising regions, and proposes refined samples.

We compare the 100 L-BFGS-B optimization runs from [15] against 5 runs of the LLM agent. The results for minimizing RMI are shown in Figure 7 and the results for maximizing RMI are shown in Figure 6. Each L-BFGS-B line starts from a random point within the design space. The best observed RMI value is plotted against the total number of function evaluations.

In all 5 runs when minimizing the RMI, the agent reaches the global optimum (objective 9) in less than 40 evaluations, matching the overall multi-start gradient-based optimization, while providing interpretable reasoning. The agent also appears to significantly outperform a single gradient-based optimization by typically finding a better optimum in fewer function evaluations. Maximizing RMI appears to be a much easier gradient-based optimization problem. The agent runs tend to converge to a common optimum (objective 277) that many of the gradient-based optimizations find, but they fail to find the global optimum.

3) *Agent Reasoning Trace*: The agent’s reasoning across three rounds reveals how it discovers the optimal configuration through systematic exploration and analysis (Figure 8).

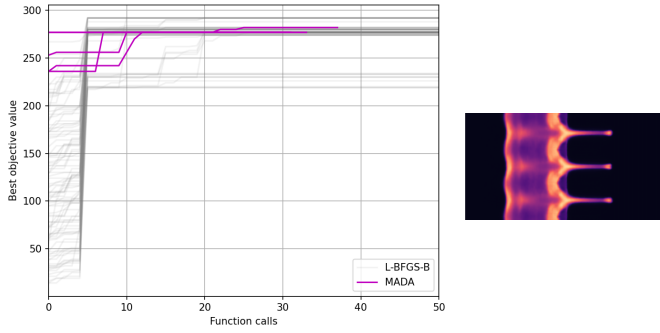


Fig. 6. Maximizing RMI: comparison of 100 L-BFGS-B optimization runs against 5 MADA runs. Each line shows the best objective versus number of evaluations (higher is better). MADA converges to a strong local optimum (objective 277). Right: density field for the best configuration found by MADA.

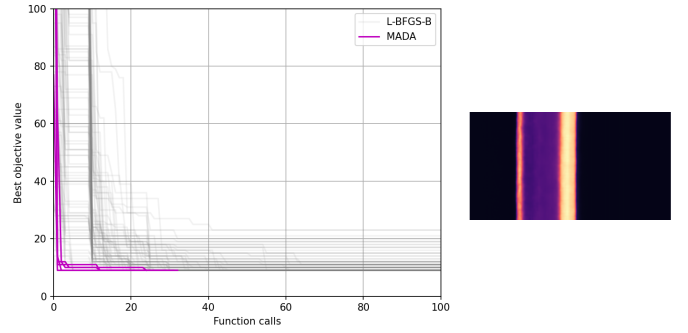


Fig. 7. Minimizing RMI: comparison of 100 L-BFGS-B optimization runs against 5 MADA runs. Each line shows the best objective versus number of evaluations (lower is better). MADA reaches the global optimum (objective 9) in under 40 evaluations across all runs. Right: density field for the best configuration found by MADA.

Round	Configuration $[P_1, P_2, P_3, P_4]$	Objective
1	$[-0.22, +0.22, -0.22, +0.22]$	256
1	$[+0.22, -0.22, +0.22, -0.22]$	253
1	$[+0.25, +0.25, +0.25, +0.25]$	14
1	$[0.00, 0.00, 0.00, 0.00]$	11
2	$[+0.25, -0.25, +0.25, -0.25]$	277
2	$[-0.25, +0.25, -0.25, +0.25]$	277
2	$[+0.22, -0.25, +0.25, -0.22]$	268
3	$[+0.23, -0.24, +0.25, -0.25]$	274
3	$[+0.25, -0.24, +0.25, -0.24]$	273
3	$[+0.22, -0.25, +0.22, -0.25]$	264

Fig. 8. Selected configurations from the agent’s reasoning trace. Round 1 explores diverse patterns; Round 2 identifies the optimal alternating configuration; Round 3 confirms the boundary optimum.

a) *Round 1: Initial Exploration.*: The agent proposes 10 diverse configurations including alternating signs, uniform values, and mixed patterns. After evaluation, it analyzes:

“Large alternating signs dominate. The two best cases are strictly alternating ± 0.22 , producing objective ≈ 250 —an order of magnitude higher than uniform cases. Magnitude alone isn’t enough: all-positive $[+0.25, +0.25, +0.25, +0.25]$ and all-negative give very weak RMI (≈ 11 – 14). Therefore, merely big P_i does not guarantee strong mixing—sign variation is critical.”

b) *Round 2: Focused Search.*: Based on Round 1 insights, the agent targets alternating patterns with large magnitudes. After evaluation:

“Magnitude matters: pushing $|P_i|$ to the upper bound (0.25) in an alternating \pm pattern produces the highest objectives (≈ 270 +). The best values sit on the boundary of the admissible range. 277 might already be close to the global maximum.”

c) *Round 3: Local Refinement.*: The agent tests micro-perturbations around the champion:

“The global champion remains the fully-maximized alternating pattern ($|P_i| = 0.25$ with strict \pm alternation). Micro-perturbations ($|P_i| \approx 0.22$ – 0.24) sit consistently in 270–274 range—close but never exceed 277. Objective appears to plateau near the boundary; perfect symmetry/alignment at the extrema delivers the highest mixing.”

The agent’s final recommendation for maximizing RMI: $P = [+0.25, -0.25, +0.25, -0.25]$ or $[-0.25, +0.25, -0.25, +0.25]$.

This evaluation demonstrates that MADA can effectively explore design spaces using surrogate models. The agent discovers that sign alternation drives RMI growth. This capability to generate explanations alongside solutions distinguishes MADA from traditional optimization approaches.

V. DISCUSSION

While MADA provides a practical approach for automated design exploration, several opportunities for future improvement remain.

Analysis limited to sampled configurations: MADA explores the design space through sampling rather than exhaustive or gradient-based search. Our approach does not guarantee finding the global optimum. However, the iterative refinement approach enables the IDA to focus sampling on promising regions identified in earlier rounds. Domain experts can also guide exploration through natural language feedback at any point in the workflow.

LLM reasoning variability: The IDA relies on LLM reasoning to analyze results and propose new configurations. As with any stochastic model, different runs may lead to variations in sampling strategies or final recommendations. We address this to some extent by recording the reasoning traces that allow experts to verify the agent’s logic.

Simulation code integration: Each simulation code requires an MCP server that exposes tools for staging and configuring simulations. Adding MCP servers to new simulation codes requires some initial development effort. However, we designed these servers to be reusable across studies, and the modular architecture allows new codes to integrate without modifying the core MADA system.

Cost of HPC simulations: Design exploration still requires running many simulations, consuming computational resources. We can mitigate this cost through surrogate models when available. The agent’s reasoning also minimizes redundant evaluations by learning from previous rounds.

VI. RELATED WORK

Recent work has explored the application of LLMs to scientific computing and discovery. ChemCrow [8] demonstrated how LLM-based agents can automate chemical research by integrating computational chemistry tools, while Boiko et al. [7] developed an autonomous laboratory system where LLMs control physical experiments through robotic platforms. In materials science, LLMs were applied for property prediction and inverse design [55], [56]. In the fusion context, a multi-agent system was used to optimize fusion target design [57].

Toward more general-purpose systems, several efforts have shown how LLM-based agents could support broader scientific and engineering workflows. Google’s AI Co-Scientist [58], a multi-agent system built on Gemini 2.0, generated novel research hypotheses and proposals, reducing hypothesis generation time from weeks to days and validating drug repurposing candidates for acute myeloid leukemia. AlphaEvolve [59] combined evolutionary search with LLMs to design advanced algorithms, discovering improved matrix multiplication methods and optimizing Google’s data center scheduling. Similarly, Cheng et al. [60] showed that LLM-based evolutionary search can match or exceed human-designed algorithms for systems problems like scheduling and load balancing. More recently, URSA framework [61] introduced a universal research and scientific agent that demonstrates the potential of AI-powered agents in automating scientific research workflows. These efforts demonstrate the growing capability of LLM-based agents to accelerate scientific discovery across diverse domains.

Multi-agent frameworks have gained traction for complex problem-solving. AutoGen [33] provides a framework for building conversational multi-agent systems, which we extend for HPC environments. CAMEL [34] explores role-playing between agents for task completion, while MetaGPT [31] structures multi-agent collaboration like a software company. Similarly, AgentVerse [32] and ChatDev [36] apply multi-agent approaches for software development tasks.

In HPC contexts, workflow management systems like Pegasus [1], Merlin [62], Swift [2], and Fireworks [3] have long automated computational pipelines. However, these systems typically require explicit workflow definitions and lack the adaptive capabilities of LLM-based approaches.

Our work differs from existing approaches by combining multi-agent LLM systems with HPC workflow management. By leveraging MCP for tool integration, we enable agents to interact directly with existing simulation codes, schedulers, and domain-specific tools. In addition, we focus specifically on iterative design optimization workflows in scientific computing. This integration enables dynamic adaptation, natural language interaction, and intelligent orchestration of complex computational workflows that would be difficult to achieve with traditional workflow systems or single-agent approaches.

VII. CONCLUSION

Scientific design workflows have traditionally required researchers to manually coordinate simulations, analyze results,

and iterate on designs. As a result, this process is often time-consuming and error-prone. The primary goal of our work was to provide a scalable approach for automating scientific design workflows on HPC systems. To achieve this, we designed an LLM-based Multi-Agent Design Assistant (MADA) where specialized agents handle distinct aspects of the design loop. Specifically, the Job Management Agent submits and monitors simulations on HPC systems, the Geometry Agent generates meshes through Cubit, and the Inverse Design Agent reasons about which configurations to explore next.

We evaluated MADA on two Richtmyer-Meshkov instability problems. We found that MADA is able to carry out iterative design refinement with minimal human intervention. MADA orchestrated mesh generation, job submission, execution of Laghos simulations on HPC systems, and result analysis to identify interface geometries that suppress RMI. Moreover, for high-velocity copper impact scenario, the Inverse Design Agent used the surrogate model to rapidly find the global optimum. Beyond the design outcome itself, the agent’s reasoning traces provided interpretable insights into the design space exploration process. Most importantly, by integrating with existing HPC infrastructure and tools while streamlining complex workflows, MADA helps scientists spend more time on scientific insight and less on orchestration, ultimately accelerating scientific discovery.

VIII. ACKNOWLEDGEMENT

This work was performed under the auspices of the U.S. Department of Energy (DOE) by Lawrence Livermore National Laboratory under Contract DE-AC52-07NA27344 (LLNL-JRNL-2016041).

REFERENCES

- [1] E. Deelman, K. Vahi, G. Juve, M. Rynge, S. Callaghan, P. J. Maechling, R. Mayani, W. Chen, R. F. Da Silva, M. Livny *et al.*, “Pegasus, a workflow management system for science automation,” *Future Generation Computer Systems*, vol. 46, pp. 17–35, 2015.
- [2] M. Wilde, M. Hategan, J. M. Wozniak, B. Clifford, D. S. Katz, and I. Foster, “Swift: A language for distributed parallel scripting,” *Parallel Computing*, vol. 37, no. 9, pp. 633–652, 2011.
- [3] A. Jain, S. P. Ong, W. Chen, B. Medasani, X. Qu, M. Kocher, M. Brafman, G. Petretto, G.-M. Rignanese, G. Hautier *et al.*, “Fireworks: a dynamic workflow system designed for high-throughput applications,” *Concurrency and Computation: Practice and Experience*, vol. 27, no. 17, pp. 5037–5059, 2015.
- [4] T. Brown, B. Mann, N. Ryder, M. Subbiah, J. D. Kaplan, P. Dhariwal, A. Neelakantan, P. Shyam, G. Sastry, A. Askell *et al.*, “Language models are few-shot learners,” pp. 1877–1901, 2020.
- [5] J. Achiam, S. Adler, S. Agarwal, L. Ahmad, I. Akkaya, F. L. Aleman, D. Almeida, J. Altenschmidt, S. Altman, S. Anadkat *et al.*, “Gpt-4 technical report,” *arXiv preprint arXiv:2303.08774*, 2023.
- [6] J. Wei, X. Wang, D. Schuurmans, M. Bosma, F. Xia, E. Chi, Q. V. Le, D. Zhou *et al.*, “Chain-of-thought prompting elicits reasoning in large language models,” *Advances in neural information processing systems*, vol. 35, pp. 24 824–24 837, 2022.
- [7] D. A. Boiko, R. MacKnight, B. Kline, and G. Gomes, “Autonomous chemical research with large language models,” *Nature*, vol. 624, no. 7992, pp. 570–578, 2023.
- [8] A. M. Bran, S. Cox, O. Schilter, C. Baldassari, A. D. White, and P. Schwaller, “Chemcrow: Augmenting large-language models with chemistry tools,” *arXiv preprint arXiv:2304.05376*, 2023.
- [9] R. Taylor, M. Kardas, G. Cucurull, T. Scialom, A. Hartshorn, E. Saravia, A. Poulton, V. Kerkez, and R. Stojnic, “Galactica: A large language model for science,” *arXiv preprint arXiv:2211.09085*, 2022.

- [10] W. Schill, M. Armstrong, J. Nguyen, D. Sterbentz, D. White, L. Benedict, R. Rieben, A. Hoff, H. Lorenzana, J. Belof *et al.*, "Suppression of richtmyer-meshkov instability via special pairs of shocks and phase transitions," *Physical Review Letters*, vol. 132, no. 2, p. 024001, 2024.
- [11] D. H. Ahn, N. Bass, A. Chu, J. Garlick, M. Grondona, S. Herbein, H. I. Ingólfsson, J. Koning, T. Patki, T. R. Scogland *et al.*, "Flux: Overcoming scheduling challenges for exascale workflows," *Future Generation Computer Systems*, vol. 110, pp. 202–213, 2020.
- [12] T. D. Blacker, S. J. Owen, M. L. Staten, W. R. Quadros, B. Hanks, B. W. Clark, R. J. Meyers, C. Ernst, K. Merkley, R. Morris *et al.*, "Cubit: Geometry and mesh generation toolkit (15.1 user documentation)," Sandia National Lab.(SNL-NM), Albuquerque, NM (United States), Tech. Rep., 2016.
- [13] Anthropic. (2024) Model context protocol. [Online]. Available: <https://modelcontextprotocol.io>
- [14] V. A. Dobrev, T. V. Kolev, and R. N. Rieben, "High-order curvilinear finite element methods for lagrangian hydrodynamics," *SIAM Journal on Scientific Computing*, vol. 34, no. 5, pp. B606–B641, 2012.
- [15] C. Jekel, D. Sterbentz, T. Stütt, P. Mocz, R. Rieben, D. White, and J. Belof, "Machine learning visualization tool for exploring parameterized hydrodynamics," *Machine Learning: Science and Technology*, vol. 5, no. 4, p. 045048, 2024.
- [16] H. Touvron, T. Lavril, G. Izacard, X. Martinet, M.-A. Lachaux, T. Lacroix, B. Rozière, N. Goyal, E. Hambro, F. Azhar *et al.*, "Llama: Open and efficient foundation language models," *arXiv preprint arXiv:2302.13971*, 2023.
- [17] S. Yao, J. Zhao, D. Yu, N. Du, I. Shafraan, K. Narasimhan, and Y. Cao, "React: Synergizing reasoning and acting in language models," in *11th International Conference on Learning Representations, ICLR 2023*, 2023.
- [18] N. Shinn, F. Cassano, A. Gopinath, K. Narasimhan, and S. Yao, "Reflection: Language agents with verbal reinforcement learning," *Advances in Neural Information Processing Systems*, vol. 36, pp. 8634–8652, 2023.
- [19] X. Wang, Z. Hu, P. Lu, Y. Zhu, J. Zhang, S. Subramaniam, A. R. Looma, S. Zhang, Y. Sun, and W. Wang, "Scibench: Evaluating college-level scientific problem-solving abilities of large language models," *arXiv preprint arXiv:2307.10635*, 2023.
- [20] S. Russell and P. Norvig, *Artificial intelligence: a modern approach*. Prentice Hall, 2010.
- [21] T. Schick, J. Dwivedi-Yu, R. Dessì, R. Raileanu, M. Lomeli, E. Hambro, L. Zettlemoyer, N. Cancedda, and T. Scialom, "Toolformer: Language models can teach themselves to use tools," *Advances in Neural Information Processing Systems*, vol. 36, pp. 68 539–68 551, 2023.
- [22] Y. Qin, S. Liang, Y. Ye, K. Zhu, L. Yan, Y. Lu, Y. Lin, X. Cong, X. Tang, B. Qian *et al.*, "Toollm: Facilitating large language models to master 16000+ real-world apis," *arXiv preprint arXiv:2307.16789*, 2023.
- [23] S. G. Patil, T. Zhang, X. Wang, and J. E. Gonzalez, "Gorilla: Large language model connected with massive apis," *Advances in Neural Information Processing Systems*, vol. 37, pp. 126 544–126 565, 2024.
- [24] G. Wang, Y. Xie, Y. Jiang, A. Mandlekar, C. Xiao, Y. Zhu, L. Fan, and A. Anandkumar, "Voyager: An open-ended embodied agent with large language models," *arXiv preprint arXiv:2305.16291*, 2023.
- [25] J. S. Park, J. O'Brien, C. J. Cai, M. R. Morris, P. Liang, and M. S. Bernstein, "Generative agents: Interactive simulacra of human behavior," in *Proceedings of the 36th annual acm symposium on user interface software and technology*, 2023, pp. 1–22.
- [26] J. Ruan, Y. Chen, B. Zhang, Z. Xu, T. Bao, H. Mao, Z. Li, X. Zeng, R. Zhao *et al.*, "Tptu: Task planning and tool usage of large language model-based ai agents," in *NeurIPS 2023 Foundation Models for Decision Making Workshop*, 2023.
- [27] J. Yang, A. Prabhakar, K. Narasimhan, and S. Yao, "Intercode: Standardizing and benchmarking interactive coding with execution feedback," *Advances in Neural Information Processing Systems*, vol. 36, pp. 23 826–23 854, 2023.
- [28] A. Madaan, N. Tandon, P. Gupta, S. Hallinan, L. Gao, S. Wiegrefe, U. Alon, N. Dziri, S. Prabhunoye, Y. Yang *et al.*, "Self-refine: Iterative refinement with self-feedback," *Advances in Neural Information Processing Systems*, vol. 36, pp. 46 534–46 594, 2023.
- [29] S. Yao, D. Yu, J. Zhao, I. Shafraan, T. Griffiths, Y. Cao, and K. Narasimhan, "Tree of thoughts: Deliberate problem solving with large language models," *Advances in neural information processing systems*, vol. 36, pp. 11 809–11 822, 2023.
- [30] S. Hao, Y. Gu, H. Ma, J. Hong, Z. Wang, D. Wang, and Z. Hu, "Reasoning with language model is planning with world model," in *Proceedings of the 2023 Conference on Empirical Methods in Natural Language Processing*, 2023, pp. 8154–8173.
- [31] S. Hong, M. Zhuge, J. Chen, X. Zheng, Y. Cheng, J. Wang, C. Zhang, Z. Wang, S. K. S. Yau, Z. Lin *et al.*, "Metagpt: Meta programming for a multi-agent collaborative framework," in *The Twelfth International Conference on Learning Representations*, 2023.
- [32] W. Chen, Y. Su, J. Zuo, C. Yang, C. Yuan, C.-M. Chan, H. Yu, Y. Lu, Y.-H. Hung, C. Qian *et al.*, "Agentverse: Facilitating multi-agent collaboration and exploring emergent behaviors," in *The Twelfth International Conference on Learning Representations*, 2023.
- [33] Q. Wu, G. Bansal, J. Zhang, Y. Wu, B. Li, E. Zhu, L. Jiang, X. Zhang, S. Zhang, J. Liu *et al.*, "Autogen: Enabling next-gen llm applications via multi-agent conversations," in *First Conference on Language Modeling*, 2024.
- [34] G. Li, H. Hammoud, H. Itani, D. Khizbullin, and B. Ghanem, "Camel: Communicative agents for "mind" exploration of large language model society," *Advances in Neural Information Processing Systems*, vol. 36, pp. 51 991–52 008, 2023.
- [35] Y. Du, S. Li, A. Torralba, J. B. Tenenbaum, and I. Mordatch, "Improving factuality and reasoning in language models through multiagent debate," in *Forty-first International Conference on Machine Learning*, 2023.
- [36] C. Qian, X. Cong, C. Yang, W. Chen, Y. Su, J. Xu, Z. Liu, and M. Sun, "Communicative agents for software development," *arXiv preprint arXiv:2307.07924*, vol. 6, no. 3, p. 1, 2023.
- [37] C. Zhang, K. Yang, S. Hu, Z. Wang, G. Li, Y. Sun, C. Zhang, Z. Zhang, A. Liu, S.-C. Zhu *et al.*, "Proagent: Building proactive cooperative ai with large language models," *CoRR*, 2023.
- [38] H. Zhang, W. Du, J. Shan, Q. Zhou, Y. Du, J. B. Tenenbaum, T. Shu, and C. Gan, "Building cooperative embodied agents modularly with large language models," *arXiv preprint arXiv:2307.02485*, 2023.
- [39] D. D. Hardin, "Pmesh: A parallel mesh generator." Lawrence Livermore National Lab., CA (United States), 10 1994. [Online]. Available: <https://www.osti.gov/biblio/79122>
- [40] CEED, "CEED/Laghos: High-Order Lagrangian Hydrodynamics Miniapp," computer software. [Online]. Available: <https://github.com/CEED/Laghos>
- [41] R. Anderson, A. Black, B. Blakeley, R. Bleile, J. Camier, J. Ciurej, A. Cook, V. Dobrev, N. Elliott, J. Grondalski *et al.*, "The multiphysics on advanced platforms project," *Technical Report No. LLNL-TR-815869*, 2020.
- [42] K. Korner *et al.*, "Differentiable lagrangian shock hydrodynamics with application to stable shock acceleration of density interfaces," Mar. 2025, arXiv preprint. [Online]. Available: <https://arxiv.org/abs/2503.17527>
- [43] J. Andrej, N. Atallah, J.-P. Bäcker, J.-S. Camier, D. Copeland, V. Dobrev, Y. Dudouit, T. Duswald, B. Keith, D. Kim, T. Kolev, B. Lazarov, K. Mittal, W. Pazner, S. Petrides, S. Shiraiwa, M. Stowell, and V. Tomov, "High-performance finite elements with MFEM," *The International Journal of High Performance Computing Applications*, vol. 38, no. 5, pp. 447–467, 2024.
- [44] C. Inc., "Chroma," Chroma Homepage, 2024. [Online]. Available: <https://docs.trychroma.com/>
- [45] S. Robertson and H. Zaragoza, "The probabilistic relevance framework: Bm25 and beyond," *Found. Trends Inf. Retr.*, vol. 3, no. 4, p. 333–389, Apr. 2009. [Online]. Available: <https://doi.org/10.1561/1500000019>
- [46] M. T. Khan, L. Chen, Y. H. Ng, W. Feng, N. Y. J. Tan, and S. K. Moon, "Leveraging vision-language models for manufacturing feature recognition in cad designs," *arXiv preprint arXiv:2411.02810*, 2024.
- [47] K. Alrashedy, P. Tambwekar, Z. Zaidi, M. Langwasser, W. Xu, and M. Gombolay, "Generating cad code with vision-language models for 3d designs," *arXiv preprint arXiv:2410.05340*, 2024.
- [48] Q. Chen, L. Li, Y. Zhang, and B. Tian, "Effects of the atwood number on the richtmyer-meshkov instability in elastic-plastic media," *Physical Review E*, vol. 99, no. 5, p. 053102, 2019.
- [49] H.-S. Park, K. Lorenz, R. Cavallo, S. Pollaine, S. Prisbrey, R. Rudd, R. Becker, . f. J. Bernier, and B. Remington, "Viscous rayleigh-taylor instability experiments at high pressure and strain rate," *Physical review letters*, vol. 104, no. 13, p. 135504, 2010.
- [50] Z. Sternberger, B. Maddox, Y. Opachich, C. Wehrenberg, R. Kraus, B. Remington, G. Randall, M. Farrell, and G. Ravichandran, "A comparative study of rayleigh-taylor and richtmyer-meshkov instabilities in 2d and 3d in tantalum," in *AIP Conference Proceedings*, vol. 1793, no. 1. AIP Publishing LLC, 2017, p. 110006.
- [51] W. Buttler, D. Oró, D. Preston, K. O. Mikaelian, F. Cherne, R. Hixson, F. Mariam, C. Morris, J. Stone, G. Terrones *et al.*, "Unstable richtmyer–

- meshkov growth of solid and liquid metals in vacuum,” *Journal of Fluid Mechanics*, vol. 703, pp. 60–84, 2012.
- [52] T. Desjardins, C. Di Stefano, T. Day, D. Schmidt, E. Merritt, F. Doss, K. Flippo, T. Cardenas, B. DeVolder, P. Donovan *et al.*, “A platform for thin-layer richtmyer-meshkov at omega and the nif,” *High Energy Density Physics*, vol. 33, p. 100705, 2019.
- [53] D. M. Sterbentz, C. F. Jekel, D. A. White, S. Aubry, H. E. Lorenzana, and J. L. Belof, “Design optimization for richtmyer–meshkov instability suppression at shock-compressed material interfaces,” *Physics of Fluids*, vol. 34, no. 8, p. 082109, 08 2022. [Online]. Available: <https://doi.org/10.1063/5.0100100>
- [54] R. Rieben, “The marbl multi-physics code,” 01 2020.
- [55] K. M. Jablonka, P. Schwaller, A. Ortega-Guerrero, and B. Smit, “Leveraging large language models for predictive chemistry,” *Nature Machine Intelligence*, vol. 6, no. 2, pp. 161–169, 2024.
- [56] S. Miret and N. M. Krishnan, “Are llms ready for real-world materials discovery?” *arXiv preprint arXiv:2402.05200*, 2024.
- [57] M. H. Shachar, D. M. Sterbentz, H. Menon, C. F. Jekel, M. G. Fernández-Godino, N. K. Brown, I. D. Boureima, Y. Hao, K. Korner, R. Rieben *et al.*, “Multi-agent design assistant for the simulation of inertial fusion energy,” *arXiv preprint arXiv:2510.17830*, 2025.
- [58] J. Gottweis and V. Natarajan, “Accelerating scientific breakthroughs with an ai co-scientist,” *Google Research Blog*, 2025.
- [59] A. Novikov, N. Vu, M. Eisenberger, E. Dupont, P.-S. Huang, A. Z. Wagner, S. Shirobokov, B. Kozlovskii, F. J. Ruiz, A. Mehrabian *et al.*, “Alphaevolve: A gemini-powered coding agent for designing advanced algorithms, 2025.”
- [60] A. Cheng, S. Liu, M. Pan, Z. Li, B. Wang, A. Krentsel, T. Xia, M. Cemri, J. Park, S. Yang *et al.*, “Barbarians at the gate: How ai is upending systems research,” *arXiv preprint arXiv:2510.06189*, 2025.
- [61] M. Grosskopf, R. Bent, R. Somasundaram, I. Michaud, A. Lui, N. Debardeleben, and E. Lawrence, “Ursa: The universal research and scientific agent,” *arXiv preprint arXiv:2506.22653*, 2025.
- [62] J. L. Peterson, K. Athey, P. Bremer, V. Castillo, F. Di Natale, J. Field, D. Fox, J. Gaffney, D. Hysom, S. Jacobs *et al.*, “Merlin: enabling machine learning-ready hpc ensembles,” Lawrence Livermore National Lab.(LLNL), Livermore, CA (United States), Tech. Rep., 2019.